ACADEMIC PRESS

Available online at www.sciencedirect.com

SCIENCE DIRECT®

Journal of Sound and Vibration 267 (2003) 605–619

JOURNAL OF SOUND AND VIBRATION

www.elsevier.com/locate/jsvi

Modelling of soil vibrations from railway tunnels

W. Gardien*, H.G. Stuit

Holland Railconsult, PO. Box 2855, 3500 GW Utrecht, Netherlands

Accepted 9 May 2003

Abstract

In densely populated areas such as the Netherlands, it is useful to predict railway traffic induced vibrations if a new railway line is to be built. A modular model, consisting of three sub-models is presented. The three sub-models are: the Static Deflection Model, the Track Model and the Propagation Model. The modular model takes into account all aspects, from the source to the propagation of waves through the soil. In order to investigate the dependence of the results on the accuracy of the model inputs, a parameter study has been performed with the third-sub model: the propagation model. For this study a Japanese metro tunnel has been modelled. Element size, soil stiffness, damping, boundary conditions and finite element method (FEM) software have been varied.

1. Introduction

In the densely populated Netherlands there is a conflict in demand for space for living, environment and infrastructure. In soft soil, as in most of the Netherlands, railway traffic generates vibrations, which propagate through the soil near the track. Railways can be built underground to save space at the surface for living and environment. However, trains running through tunnels will still generate vibrations, and these vibrations can annoy people near the track. Therefore, it is useful to predict these vibrations if a tunnel is to be built in a densely populated area.

The finite element method is a useful tool to quantify the intensity of railway traffic induced vibrations. The advantage of using a finite element approach is that the interaction between the tunnel and the surrounding soil layers can easily be modelled. A disadvantage of computing wave propagation in soil layers with finite elements is that many elements are needed to compute the

*Corresponding author. Tel.: +31-30-265-3670; fax: +31-30-265-3581.
E-mail addresses: wgardien@hr.nl, hgstuit@hr.nl (W. Gardien).

0022-460X/$ - see front matter
doi:10.1016/S0022-460X(03)00727-2

wave field properly. This might result in long computation times. However, the computation times of a two-dimensional (2D) finite element model are quite acceptable.

Unfortunately the propagation of waves generated by a train running through a tunnel is a true three-dimensional (3D) problem. The propagation behaviour in the direction of the tunnel axis is totally different from the behaviour perpendicular to the tunnel axis. A complete 3D FE analysis of a train travelling through a tunnel surrounded by soil layers is not practicable with current computer power. For that reason, a modular model has been created.

The accuracy of the results of the FE analysis depends on many parameters. The influence of one parameter might be stronger than any other. Several analyses have been made to examine the influence of the amount of damping, the stiffness of the soil, the element mesh, the boundary conditions and the choice of FEM software.

2. Description of the model

The modular model consists of three sub-models. The three sub-models are:

- The Static Deflection Model: with this static 3D FE model, the properties of the tunnel in terms of a Timoshenko beam are determined.
- The Track Model: in this model the force exerted on the tunnel during a train passage is computed.
- The Propagation Model: this model calculates the propagation of vibrations from the tunnel through the soil.

The flow chart in Fig. 1 shows the connection of the three sub-models. A more detailed description of the sub models can be found in the following paragraphs. The description comes from Ref. [1].

2.1. Static Deflection Model

This is a 3D static FE model of the tunnel and the surrounding soil layers (Fig. 2), which is used to determine the characteristics of the tunnel in terms of a Timoshenko beam. At the $y-z$ plane and the $x-y$ plane symmetry boundary conditions apply. The depth of the model should extend a long way below the bottom of the tunnel. If this not the case, the vertical stiffness of the supporting soil layers can not be determined properly. Moreover, if the width of the model is too small, the vertical stiffness of the model cannot be determined properly. In order to calculate the bending and shear stiffness of the tunnel, the length of the model should be sufficiently large.

The model is statically loaded in the vertical direction at the location of the track. As a result of this, the tunnel will deflect vertically (Fig. 3). The vertical deflection along the tunnel axis is used as input for a curve fit procedure. The bending stiffness EI, the shear stiffness Z, and the vertical stiffness k of the supporting soil layers are obtained from this curve fit procedure. These values are used as input parameters for the next sub-model.

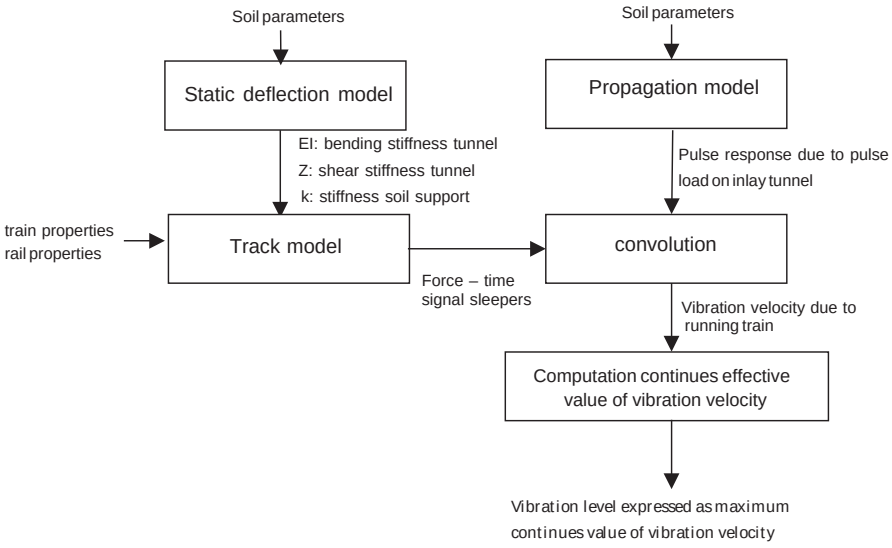

Fig. 1. Flow chart, vibration prediction model.

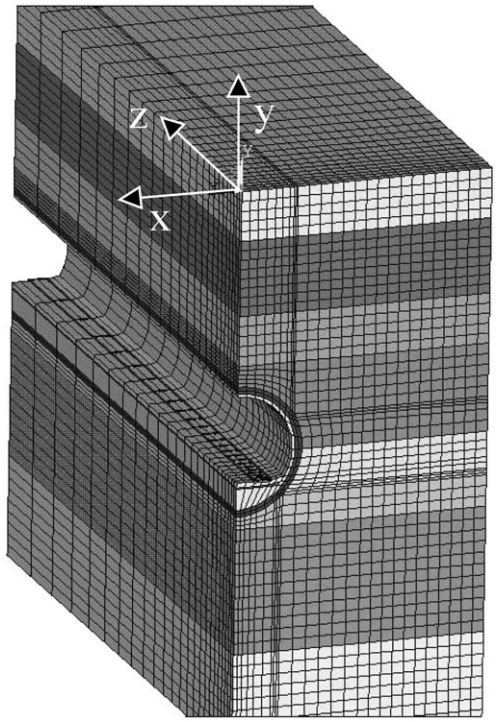

Fig. 2. Static Deflection Model.

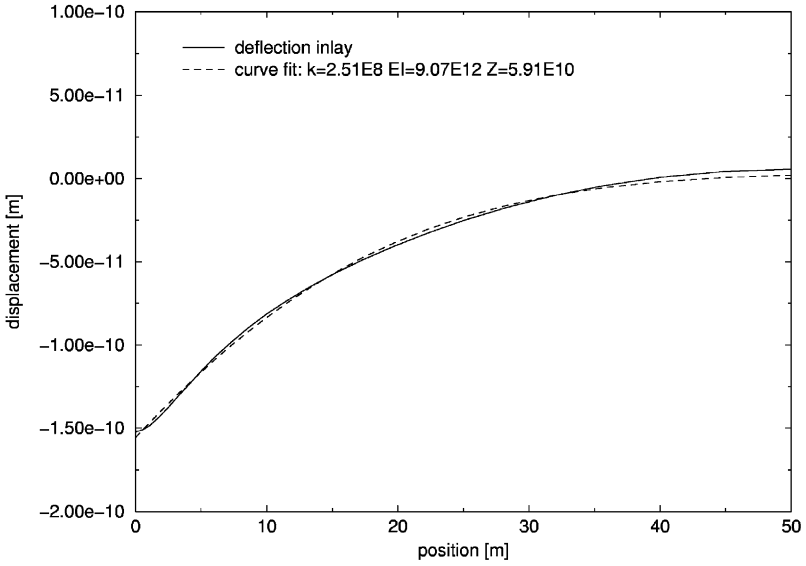

Fig. 3. Deflection of inlay tunnel and curve fit due to static load of 1 N.

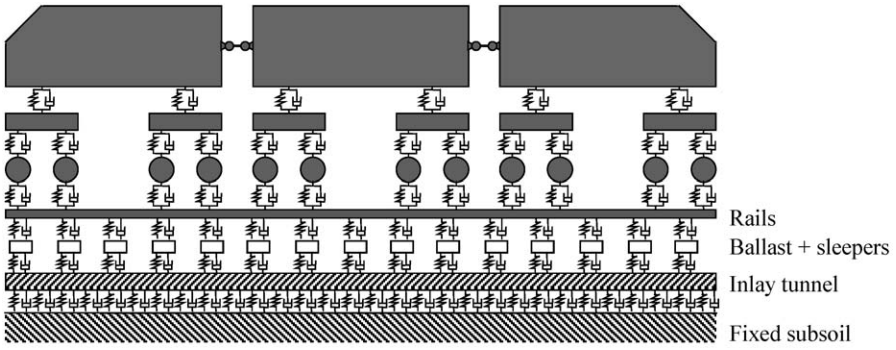

Fig. 4. Track Model.

2.2. Track Model

The Track Model (Fig. 4) calculates the response of the tunnel to a travelling train. Results from the static deflection model are used as model inputs. The tunnel and the rails are modelled as a Timoshenko beam, with both bending stiffness EI and shear stiffness Z. The ballast and the sleepers are modelled as a single mass–spring system. On the top of the rail, there is a certain rail irregularity. This irregularity is responsible for the high frequency vibrations. The train consists of coaches, bogies and axles, which are all modelled as rigid bodies. They are connected to each other by springs and dampers. Rails and axles are connected to each other by means of a non-linear Hertzian contact spring. The output of this model is the force of the spring/damper systems between the sleepers and the tunnel inlay (Fig. 5). These forces are applied as a load on the next sub-model.

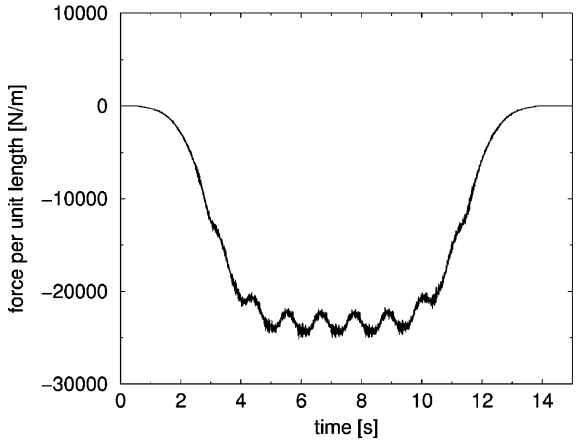

Fig. 5. Force–time signal from sleepers averaged over characteristic length.

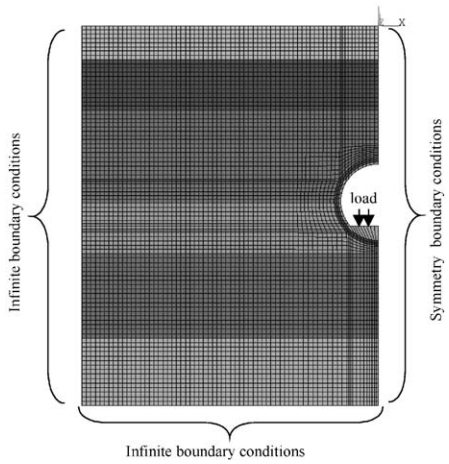

Fig. 6. Propagation Model.

2.3. Propagation Model

This FE model (Fig. 6) calculates the wave propagation from the tunnel through the soil layers. It can either be a 2D or a 3D impulse response calculation, and consists entirely of volume elements (3D) or plane strain elements (2D). The calculations are carried out in the time domain. At the vertical plane along the tunnel axis, symmetry boundary conditions apply. Infinite boundary conditions apply at the bottom and the left-hand side. These boundary conditions allow the seismic energy to disappear from the model without reflections, so that the model behaves like an infinite layered half-space. The infinite boundary conditions consist of several layers of elements with increasing size and material damping. The model is loaded by a short pulse at the position of the track. Due to this pulse, waves will propagate through the soil (Fig. 7). By

convoluting the force–time signal from the track model with the impulse response, the vibration velocities of an arbitrary point due to a running train can be computed.

In the case of a 3D propagation model, the force–time signals of all spring–damper systems (sleepers) from the track model are convoluted with the 3D impulse response. Now for each separate sleeper of the track model, the 3D response is known. The complete 3D response in the field of a running train follows from the summation of all the separate 3D sleeper responses.

If the 2D version of the propagation model is being used, the contribution of multiple sleepers is also taken into account as well. This is achieved by averaging the force–time sleeper signals over a certain characteristic length. The signal displayed in Fig. 5 is an example of an averaged signal. This average force–time signal will be applied as a load on the inlay of the 2D model. Fig. 8 shows the vibration velocity at the surface, which is the result of a convolution of the 2D impulse response with the force–time signal.

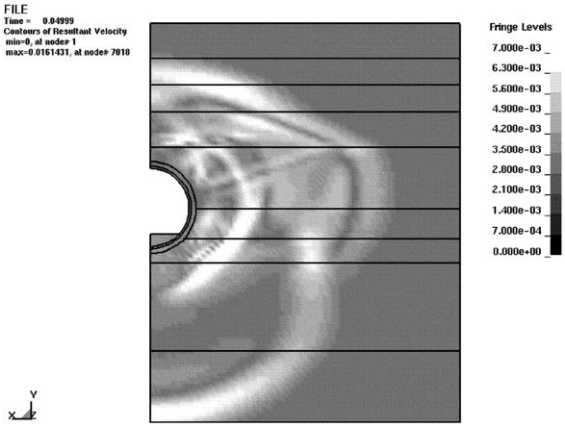

Fig. 7. Vibration velocities [m/s] due to pulse response at $t = 0.05$ s.

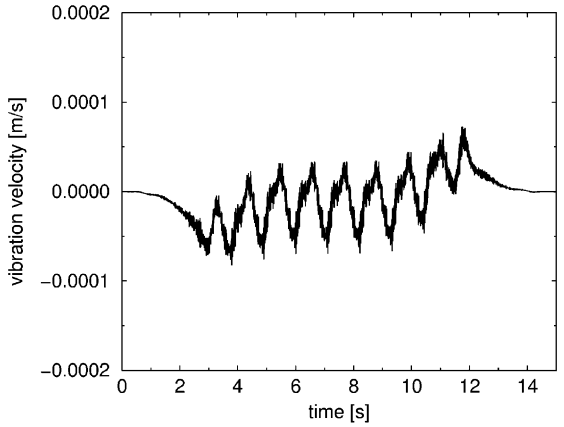

Fig. 8. Vertical vibration velocity at point.

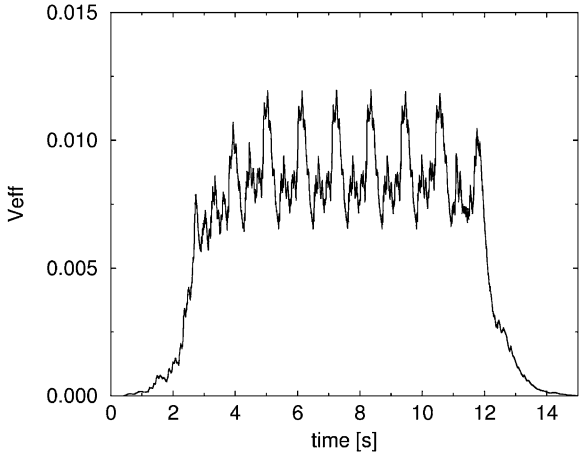

Fig. 9. Continuous effective value of vibration velocity.

In order to quantify the vibration level by one single number the maximum continuous effective value of the vibration velocity (Eq. (1)) will be computed from the vibration velocity. This is done according to SBR guideline 2 [2].

$$v_{eff}(t) = \sqrt{\frac{1}{\tau}\int_0^t \exp(-\xi/\tau)v^2(t-\xi)\,\mathrm{d}\xi} \tag{1}$$

with $\tau = 0.125\,\mathrm{s}$

The continuous effective value of this signal can be seen in Fig. 9. The maximum continuous effective value is just the maximum of this signal. As the continuous effective value is divided by 1 mm/s, the presented values are dimensionless.

3. Parameter study

The accuracy of the vibration prediction will depend on the chosen input parameters. In order to quantify the effect of a certain parameter on the results, several input parameters have been varied. The reference model for the parameter study was a model of a Japanese metro tunnel.

Vibrations from the Japanese bored metro tunnel have been predicted and measured. A detailed description of how the measurement was set up can be found in Ref. [3]. In Fig. 10 the tunnel is displayed with respect to measuring points $m1$, $m2$ and $m3$ at the surface. The top of the tunnel is 16 m below the surface. Measuring point $m1$ is located above the tunnel axis, and points $m2$ and $m3$ are horizontally 10 and 25 m away from the tunnel axis. Inside the tunnel (Fig. 11), the vibration velocities are predicted at points $t1$ (inlay between rails), $t2$ (middle of inlay) and $t3$ (tunnel lining).

The parameter study has focused on the 2D plane strain version of the propagation model. The choice of material parameters, damping, element size, boundary conditions and FEM software has been quantified. In all cases the results have been compared with the same reference model.

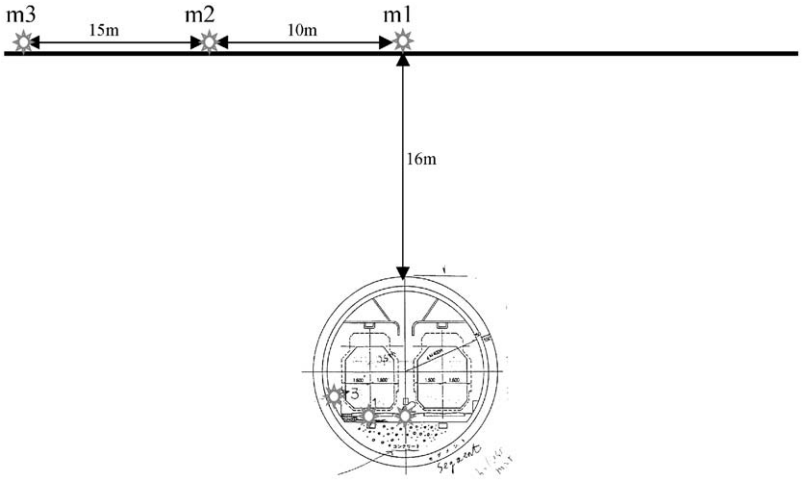

Fig. 10. Metro tunnel and measuring points.

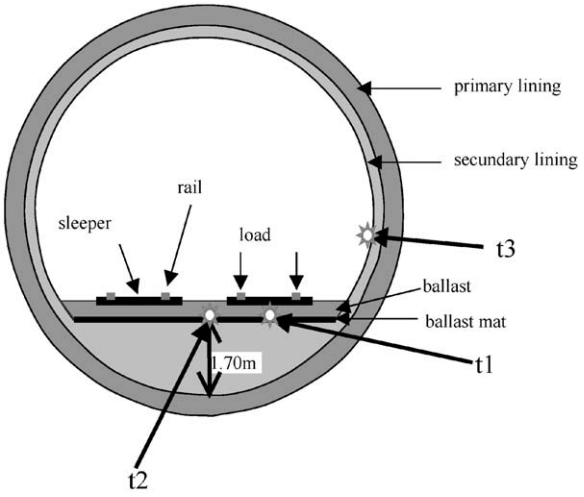

Fig. 11. Geometry of tunnel with measuring points $t1$, $t2$ and $t3$.

3.1. Material parameters

In the reference model, the material parameters of the soil are based on soil analyses. From these soil analyses, the dynamic Young's modulus of the soil layers are determined (Table 1). An error in the value of the dynamic stiffness of the soil might lead to an error in the results.

In order to investigate the effect of the material parameters on the results, the stiffness of all soil layers of the reference model have been multiplied and divided by a factor 3. As can be seen in Fig. 12, the form of the admittance–frequency curve is different, but the admittance levels do not differ much from the reference model.

Table 1
Reference material properties of soil layers

Layer #	Thickness (m)	Density (kg/m^3)	Young's modulus (N/m^2)	Poisson ratio (dimensionless)	Damping (%)
1	4	1900	30E6	0.40	2
2	3	1700	20E6	0.45	5
3	3	1700	40E6	0.45	5
4	4	1900	20E6	0.45	3
5	7	2100	200E6	0.40	2
6	3.5	1900	90E6	0.45	3
7	2.5	1600	50E6	0.45	5
8	10	1900	90E6	0.45	3
9	—	2000	130E6	0.40	2

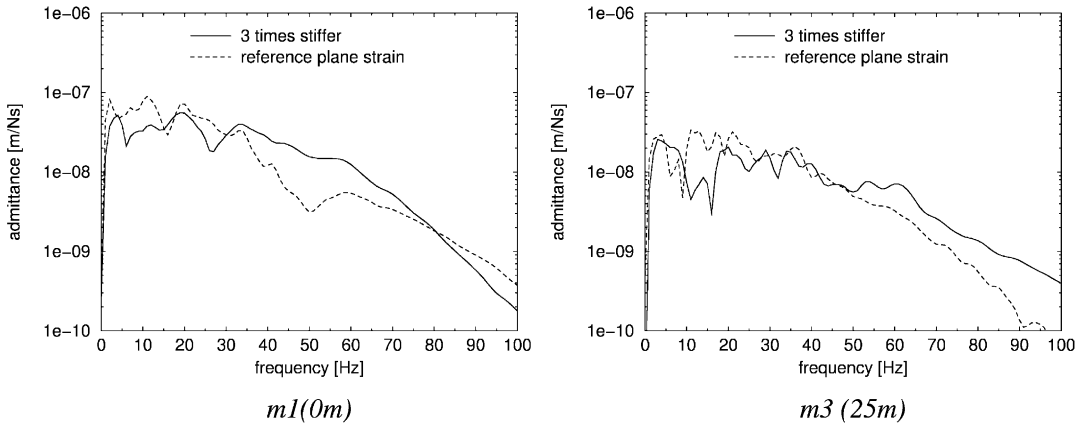

Fig. 12. Vertical admittance stiff model compared with reference mesh.

Table 2 shows the dependence of the final results on the soil parameters. At the surface, the measuring point above the tunnel axis is most sensitive to a deviation of the stiffness. At 10 and 25 m from the tunnel axis the influence of the material parameters on the results is relatively small. In the tunnel itself, all measuring points are sensitive to the value of the Young's modulus by approximately the same extent. Generally, the increase in vibration levels due to a decrease in the Young's modulus is considerably less than a linear relationship. The points close to the vibrating source are affected most by a change in material parameters.

3.2. Damping

The damping in the soil is a parameter that is difficult to determine. Often 2–5% of the critical damping is chosen as the material damping value. In the Finite Element code, the damping is defined as a combination of mass proportional and stiffness proportional damping [4]:

$$[\mathbf{C}] = \alpha[\mathbf{M}] + \beta[\mathbf{K}], \tag{2}$$

Table 2
Maximum continuous effective values (mm/s) at measuring points for reference model and models with adapted material parameters

	Surface			Tunnel		
	*m*1 0 m	*m*2 10 m	*m*3 25 m	*t*1	*t*2	*t*3 Lining
Reference material parameters	0.0098 (100%)	0.0112 (100%)	0.0039 (100%)	0.0331 (100%)	0.0283 (100%)	0.0190 (100%)
Young's modulus: 1/3∗reference	0.0188 (192%)	0.0133 (119%)	0.0043 (110%)	0.0507 (153%)	0.0381 (135%)	0.0209 (110%)
Young's modulus: 3∗reference	0.0091 (93%)	0.0088 (79%)	0.0037 (95%)	0.0187 (53%)	0.0178 (63%)	0.012 (63%)

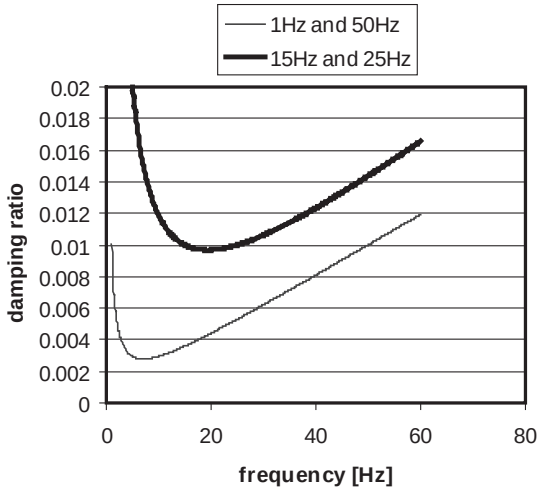

Fig. 13. Damping ratio of 0.01 (1%) dependent on frequency.

where [**K**] is the stiffness matrix, [**M**] is the mass matrix, [**C**] is the damping matrix, α is the coefficient of mass proportional damping; β is the coefficient of stiffness proportional damping

In this formulation of the damping, two frequencies can be chosen at which a given proportional damping applies. At other frequencies, the damping ratio will be different. Fig. 13 shows two cases. In the baseline case, the damping ratio is chosen so that it is exactly 1% at 15 and 25 Hz. In that case, the damping ratio is close to 1% between 15 and 25 Hz. However, at lower frequencies, the damping ratio is considerably larger. The two values at which the damping ratio will match the given value should not be too far away from each other. In Fig. 13 can be seen that the damping ratio will drop to 0.3% if the lower and upper bounds are 1 and 50 Hz.

The influence of the damping on the vertical admittance at measuring point *m*3, is larger than at measuring point *m*1 (Fig. 14). Over the whole frequency range the admittance will increase if the damping ratio has a smaller value. The effect of the damping on the final results is shown in Table 3. At the surface, points far away from tunnel are affected most by the damping. The

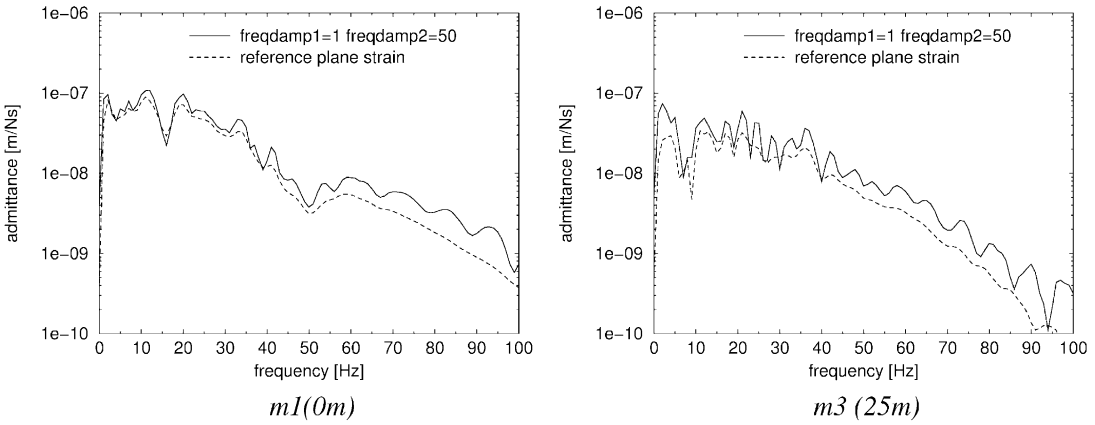

Fig. 14. Vertical admittance model with small values of relative damping compared with reference model.

Table 3
Continuous effective values (mm/s) at measuring points for reference model and models with adapted relative damping

	Surface			Tunnel		
	*m*1 0 m	*m*2 10 m	*m*3 25 m	*t*1	*t*2	*t*3 Lining
Reference: 15 and 25 Hz	0.0098 (100%)	0.0112 (100%)	0.0039 (100%)	0.0331 (100%)	0.0283 (100%)	0.0190 (100%)
Relative damping 5 and 50 Hz	0.0118 (120%)	0.0146 (130%)	0.0054 (138%)	0.0328 (99%)	0.0289 (102%)	0.0192 (101%)
Relative damping 1 and 50 Hz	0.0148 (151%)	0.0172 (154%)	0.0091 (233%)	0.0336 (102%)	0.0299 (106%)	0.0212 (112%)

influence of the damping on the results inside the tunnel is negligible compared to the influence at the surface.

3.3. Element size

The element size in the propagation model is based on the wavelength of the Rayleigh wave. The Rayleigh wave is often the dominant type of wave generated by railway traffic. Experience with vibration prediction studies showed that one Rayleigh wavelength should be described by at least 8 elements [5]. In the reference model the element size is based on a Rayleigh wave with a maximum frequency of 15 Hz.

In Fig. 15 the admittance of the reference 2D propagation model has been compared with the admittance of a model with an element size based on a Rayleigh wave with a frequency of 5 Hz. Clearly, the coarser 5 Hz mesh will lead to a smaller admittance at the higher frequencies, but the deviation starts at frequencies much higher than 5 Hz. In this case, compression and shear waves play a more important role than Rayleigh waves [6]. A compression wave has a much longer

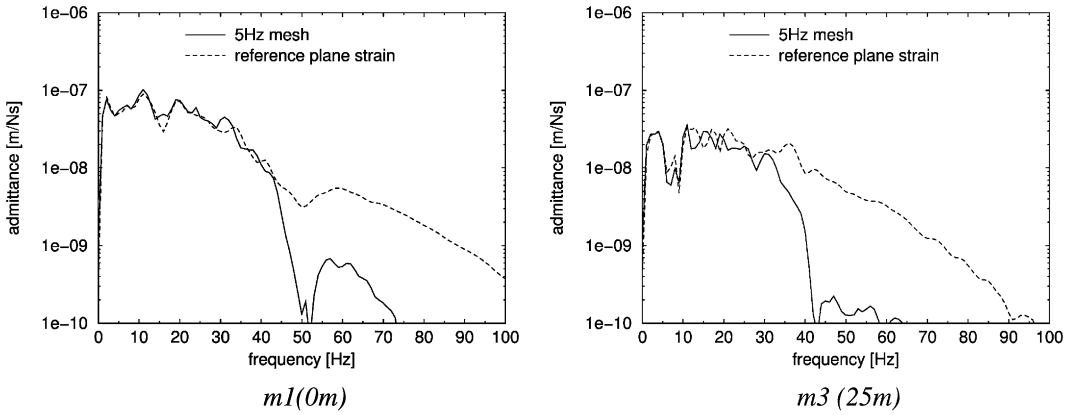

Fig. 15. Vertical admittance of coarse mesh compared with reference mesh.

Table 4
Maximum continuous effective values (mm/s) at measuring points for reference mesh, coarse mesh and fine mesh

	Surface			Tunnel		
	$m1$ 0 m	$m2$ 10 m	$m3$ 25 m	$t1$	$t2$	$t3$ Lining
Reference (15 Hz)	0.0098	0.0112	0.0039	0.0331	0.0283	0.0190
Element size = 0.452 m	(100%)	(100%)	(100%)	(100%)	(100%)	(100%)
Coarse mesh (5 Hz)	0.0097	0.0077	0.0037	0.0282	0.0255	0.0204
Element size = 1.36 m	(99%)	(69%)	(95%)	(85%)	(90%)	(107%)
Fine mesh (50 Hz)	0.0095	0.012	0.0041	0.0313	0.0275	0.0184
Element size = 0.136 m	(97%)	(107%)	(105%)	(95%)	(97%)	(97%)

wavelength than a Rayleigh wave. Therefore, at frequencies higher than 5 Hz compression waves will still be represented well in the coarse mesh.

The admittance at measuring point $m1$ starts to deviate from the admittance of the reference model at a frequency of approximately 40 Hz. At $m3$, the admittance of the 5 Hz mesh already deviates from the reference model at 30 Hz. So, if the mesh chosen is too coarse, the loss of high frequencies will first be noticeable at greater distances.

The effect of the element size on the results is shown in Table 4. In general, a coarse mesh will lead to lower vibration levels at the surface. In this case, a fine mesh is not much more accurate than the reference mesh.

3.4. Boundary conditions

The reference model uses special boundary conditions to allow the seismic energy to disappear from the model. If the boundaries were fixed, the different propagating waves in the model would reflect at the fixed boundaries. This would probably lead to stronger vibrations.

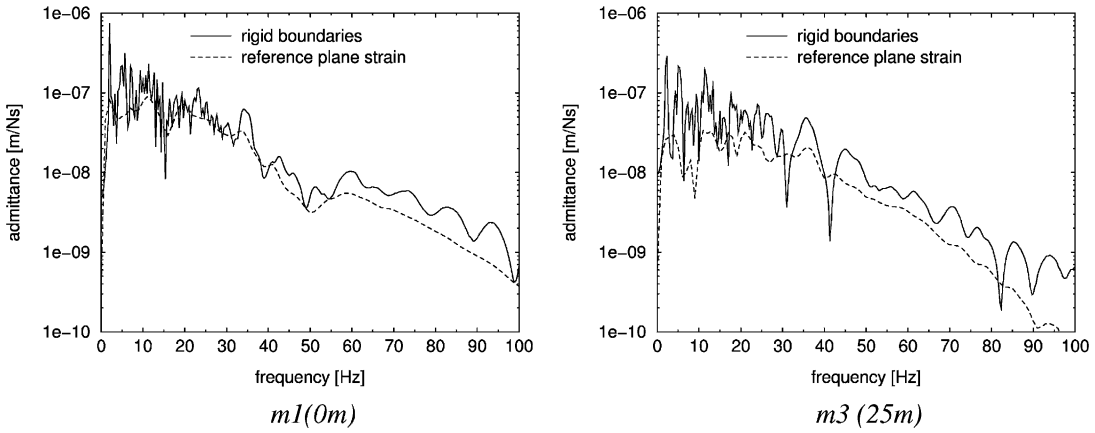

Fig. 16. Vertical admittance model with fixed boundary conditions compared with reference model.

Table 5
Continuous effective values (mm/s) at measuring points for reference model and model with rigid boundaries

	Surface			Tunnel		
	*m*1 0 m	*m*2 10 m	*m*3 25 m	*t*1	*t*2	*t*3 Lining
Reference: Non-reflecting boundaries	0.0098 (100%)	0.0112 (100%)	0.0039 (100%)	0.0331 (100%)	0.0283 (100%)	0.0190 (100%)
Relative damping	0.0189	0.0164	0.0076	0.0308	0.0270	0.0169
Rigid boundaries	(193%)	(146%)	(195%)	(93%)	(95%)	(89%)

Fig. 16 shows that the average admittance levels for a model with fixed boundary conditions are higher than for a model with non-reflecting boundaries. Furthermore the admittance curve contains many more peaks and dips than the admittance curve of the reference model. The values in Table 5 confirm that fixed boundaries will lead to higher vibration levels.

3.5. FEM software

The impulse response of the propagation model has been carried out using the LS-DYNA FEM software. LS-DYNA uses an explicit time integration scheme to compute the solution. In order to find out to what extent the choice of the FEM software influences the results, the same predictions have been made with ANSYS. The ANSYS FEM software uses an implicit time integration scheme. In ANSYS, the only way to incorporate alpha damping is by defining a global alpha damping. The alpha damping used in the ANSYS model is the average alpha damping of the soil layers. Furthermore, the effectiveness of the non-reflecting boundaries depends on the alpha damping. For that reason, some differences can be expected, especially at greater distances.

In Fig. 17 the admittance of the LS-DYNA model is compared with the ANSYS model. At frequencies under 40 Hz the differences are small. At higher frequencies, the differences increase. In this case, frequencies under 40 Hz are dominant. Therefore, the influence on the final results is

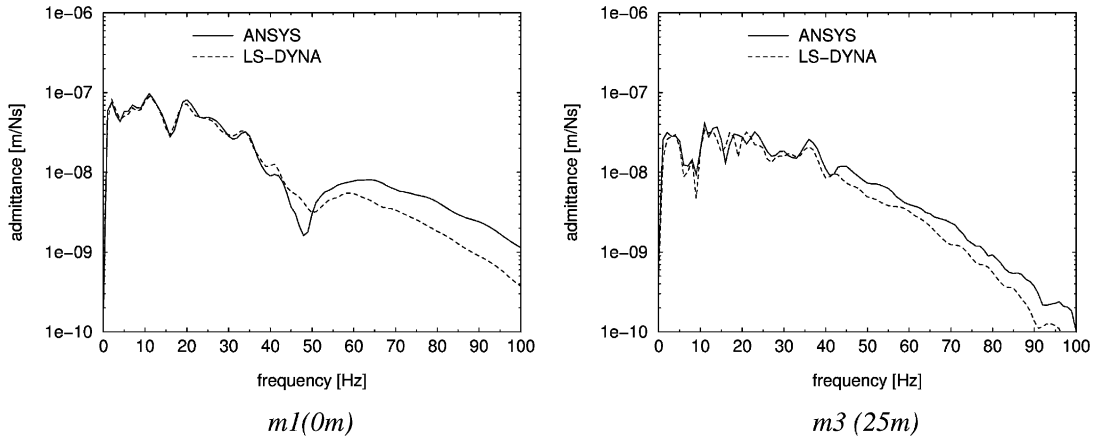

Fig. 17. Vertical admittance LS-DYNA model and ANSYS model.

Table 6
Continuous effective values (mm/s) at measuring points for LS-DYNA model and ANSYS models

	Surface			Tunnel		
	*m*1 0 m	*m*2 10 m	*m*3 25 m	*t*1	*t*2	*t*3 Lining
Reference: LS-DYNA	0.0098 (100%)	0.0112 (100%)	0.0039 (100%)	0.0331 (100%)	0.0283 (100%)	0.0190 (100%)
ANSYS	0.0112 (114%)	0.0128 (114%)	0.0051 (130%)	0.0407 (123%)	0.0307 (108%)	0.0196 (103%)

small. Given the fact that some differences can be expected, the differences between the results of the ANSYS model and the results of the LS-DYNA model are small (Table 6).

4. Conclusions

The finite element method (FEM) is a suitable tool to predict vibrations generated by rail traffic. Vibrations generated by a train travelling in a tunnel are a true 3D phenomenon. Unfortunately, a complete 3D FEM model that contains all aspects is not currently feasible because of computer power. Therefore a model that consists of 3 sub-models is presented. The model takes into account all important aspects that play a role in the generation of vibrations.

The following conclusions can be drawn from the parameter study:

4.1. Material parameters

The material parameter that can vary most is Young's modulus. Close to the tunnel a stiffer model will lead to larger vibration levels and vice versa. Further away from the tunnel a different

Young's modulus has less influence on the results. If the Young's modulus increases by a factor of 2, the vibration levels will decrease by less than a factor of 2.

4.2. Damping

In the Finite Element formulation the damping is defined as a combination of mass and stiffness proportional damping. The frequency at which the damping ratio applies should be chosen with care. If the chosen frequency range is wide, the damping will be small between the lower and upper bound frequencies. Close to the tunnel, damping has a minor influence at the results, but further away, damping will play a very important role.

4.3. Element size

In order to represent a wavelength correctly, a sufficient number of elements should be chosen. Generally, the vibration levels will be lower if too coarse a mesh is chosen. In the case of the tunnel, the admittance of the 5 Hz (coarse) mesh was roughly the same as the reference mesh up to frequencies of 30 Hz. The element size is based on the Rayleigh wavelength at a certain frequency, but probably in this case compression waves played a more important role.

4.4. Boundary conditions

The reference model uses non-reflecting boundaries to let the seismic energy disappear from the model. If the boundaries are fixed, strong reflections will occur, and vibration levels can be higher by up to a factor of 2. In reality, this can happen if a thick layer of bedrock supports soft soil.

4.5. FEM software

The parameter study has been carried out using the explicit time integration LS-DYNA FEM software. If the computations are made with the implicit time integration ANSYS FEM software, the differences are small. Therefore the choice of FEM software should not have much influence on the results.

The parameter study has focused on the 2D version of the propagation model. In future work the parameter study will be extended to the static deflection model and the track model in order to quantify the influence of all important input parameters.

References

[1] W. Gardien, Verslag Workshop Benchmark studie. Holland Railconsult, Report Reference GMV-MVD-01001981\004, Utrecht, 2001.
[2] P.C. van Staalduinen, J. van der Vecht, *SBR Guideline 2—hinder voor personen in gebouwen door trillingen*, Stichting Bouwresearch, Rotterdam, ISBN 90-5367-080-7.
[3] P. Hölscher, Measurements at Shinjuku line Tokyo, Project organization HSL-South, Report Reference NOH/140401, 2000.
[4] LSTC, LS-DYNA Keyword User's Manual (8.5), Livermore Software Technology Corporation, Livermore, 1999.
[5] W. Gardien, Aantal elementen voortplantingsmodel, Holland Railconsult Internal Report, Utrecht, 1998.
[6] C. Esveld, *Modern Railway Track* (347-352), MRT-Productions, Duisburg, 1989, ISBN 90-800324-1-7.